Controlled crack patterns in thin brittle layers

Roland Szatmári and Ferenc Kun

Department of Theoretical Physics, University of Debrecen, P.O. Box 5,
H-4010 Debrecen, Hungary

Motivation

Shrinkage induced cracking of thin material layers attached to a rigid substrate is abundant in nature giving rise to the formation of spectacular polygonal crack patterns. Examples can be mentioned on a wide range of length scales from dried lake beds through permafrost regions on Earth and Mars, to the three-dimensional structures of coloumnar joints formed in cooling volcanic lava.

It is a great challange to control the structure of shrinkage induced two-dimensional crack patterns also due to its high importance for technological applications. Recently, it has been demonstrated experimentally for dense calcium carbonate and magnesium carbonate hydroxide pastes that applying mechanical excitation by means of vibration or flow of the paste the emerging desiccation crack pattern remembers the direction of excitation, i.e. main cracks get aligned and their orientation can be tuned by the direction of mechanical excitation (Fig. 1).

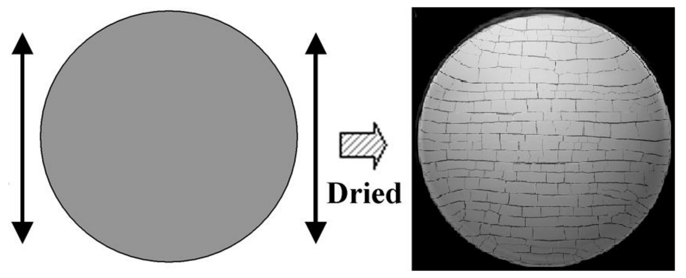

Fig. 1. Lamellar crack pattern which appears when the container is initially vibrated in one direction.

Discrete Element Model

In order to understand the mechanism of this memory effect, we studied the process of shrinkage induced cracking by means of realistic discrete element simulations. In the model a thin layer is discretized on a random lattice of Voronoi polygons attached to a substrate. To represent the mechanics of the layer the center of mass of neighbouring polygons are connected by breakable beam elements. In order to capture the adhesion of the layer to the substrate material the polygons are coupled to underlaying plane by initially stress free spring elements. To capture the effect of shrinking in the model the natural length of beams is gradually decreased as a function of time. As the system evolves, this shrinkage gives rise to a homogeneous deformation field, where overstressed beams break creating cracks in the layer. We impose a breaking rule which can reflect the fact that the longer and thinner beams are easier to break,

$$\left(\frac{\varepsilon_{ij}}{\varepsilon_{th}}\right)^2 + \frac{\max\left(|\theta^i|, |\theta^j|\right)}{\theta_{th}} \geq 1.$$

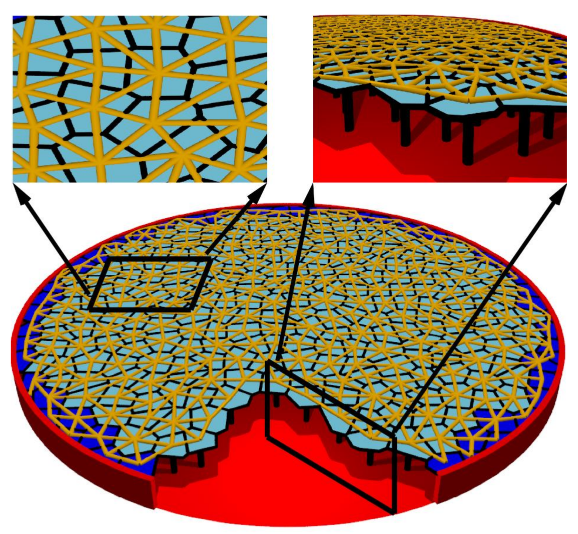

Fig. 2. Main components of the model construction: the shrinking layer is discretized in terms of convex polygons. The polygons and beams (yellow lines) in between represent material elements and their cohesive breakable contacts, respectively. The adhesion of the layer is captured by spring coupling the center of polygons to the substrate. The boundary polygons of the sample, highlighted by blue color, are fixed to the container wall (red cylinder around the sample).

This breaking criterion is evaluated at each iteration step and those beams which fulfill the condition are removed from the simulations.

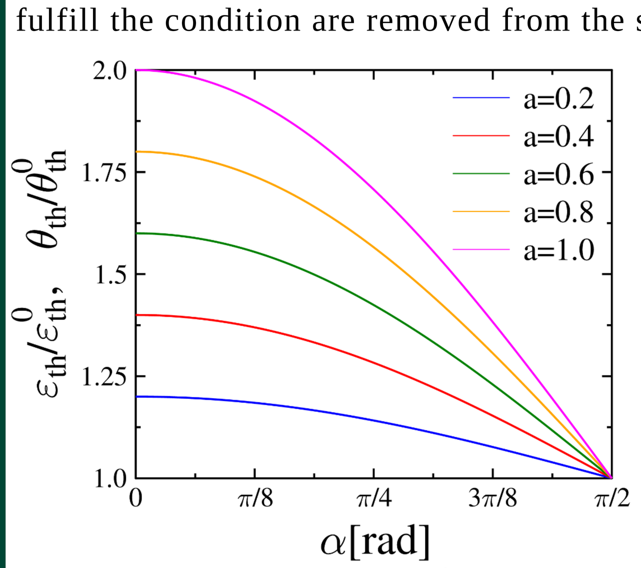

Fig. 3. Angular dependence of the breaking parameters ε_{th} and θ_{th}. The angle α is measured from the horizontal axis.

The value of the breaking parameters ε_{th} and θ_{th} control the relative importance of the stretching and bending modes of breaking. We assume that the plastic deformation imprinted by the initial mechanical excitation in pastes introduces a directional dependence of the fracture strength of the solidifying paste. In order to capture this effect in the model, the breaking thresholds do not have any randomness, however, we assume that they depend on the orientation angle α of the beam with respect to the horizontal axis, which represents e.g. the direction of shaking in the initial configuration.

For simplicity, we implemented the functional forms

$$\varepsilon_{th}(\alpha) = \varepsilon_{th}^0(1 + a\cos\alpha),$$
$$\theta_{th}(\alpha) = \theta_{th}^0(1 + a\cos\alpha),$$

where the orientation angle α takes values in the range $0 \leq \alpha \leq \pi/2$ (Fig. 3).

Breaking mechanism

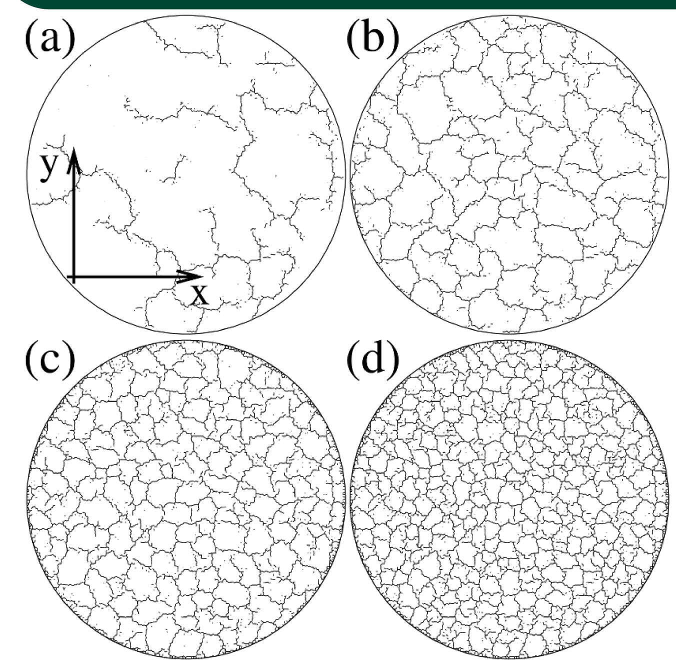

Fig. 4. Time evolution of cracking in an isotropic *a=0.0*. Snapshots are presented at different values of the fraction of broken fibers d: *(a)* 0.06, *(b)* 0.14, *(c)* 0.22 and *(d)* 0.30.

We performed a large amount of computer simulations varying the value of a in the range of $0 \leq a \leq 5$ to reveal how to anisotropy affects the evolution of the fracture process and the structure of the emerging crack network as the layer gradually shrinks. To quantify the overall damage suffered by the layer during the fracture process, we introduced the fraction of breaken bems $d(t)$ with the definition $d(t)=N_b(t)/N_B$, where N_b and N_B denote the number of beams broken up to time t and the total number of beams in the layer in the initial state, respectively. Our model contains solely a single source of disorder, i.e. the discretization of the material on a random lattice of convex polygons which introduces structural disorder without any directional dependence. Hence, for zero anisotropy $a = 0.0$ of the breaking thresholds, representing the absence of initial mechanical excitation in experiments, a cellular crack pattern is expected with a high degree of isotropy of the crack orientation. This is illustrated in Fig. 4 where snapshots of the evolution of the crack pattern are shown at $a = 0.0$ for 4 different values of hte damage parameter d. Main outcomes of the study of the isotropic case of unperturbed, homogeneous layers:

- Before bond breaking sets on the shrinkage of beams generates a nearly uniform stress field.
- The first microcracks nucleate at random positions and gradually grow (Fig. 4(a-b)).
- Fragments are formed when the entire crack network becomes connected, which occurs between Fig. 4(c) and (d).
- Further shrinking results in crack formation typically in the middle of the fragments which breaks them into two pieces gradually reducing their size.

Simulations revelaed that the presence of anisotropy $a > 0$ has a strong effect both on the initiation and propagation of cracks, which in turn shows up also in the structure of the crack pattern and in the geometrical features of fragments. This is demonstrated by Fig. 5 for the case of $a = 1.0$ presenting 4 snapshots of the evolution at different stages d of the fracture process. Due to the directional dependence of the local strength, in the initial phase of the fracture process those beams break which have a higher angle $\alpha \approx \pi/2$ with the horizontal direction. Removal of beams create microcracks along the side of polygons, which are nearly perpendicular to the beam direction. As a consequence, the primary cracks grow mainly along the horizontal direction as it can be observed in Fig. 5(a). As the strain increases in the layer with shrinking, stronger beams at a lowe angle with the horizontal direction start also to break creating cracks even along the vertical direction in Fig. 5(b). When the fully connected crack network appears, the strong alignment of cracks results in a pronounced anisotropy of the emerging fragments (Fig. 5(c)).

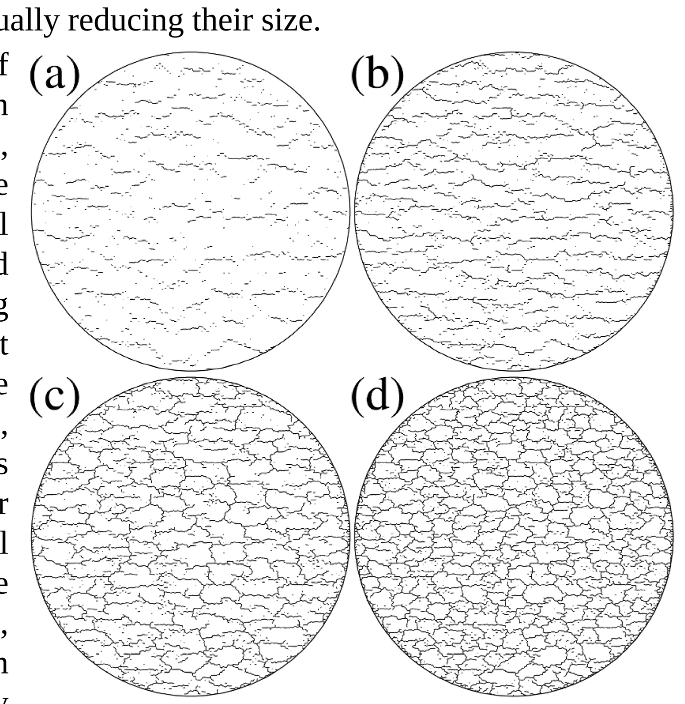

Fig. 5. Time evolution of the cracking thin layer in the presence of anisotropy a=1.0. Snapshots are presented at different values of the fraction of broken fibers d: *(a)* 0.06, *(b)* 0.14, *(c)* 0.22 and *(d)* 0.30.

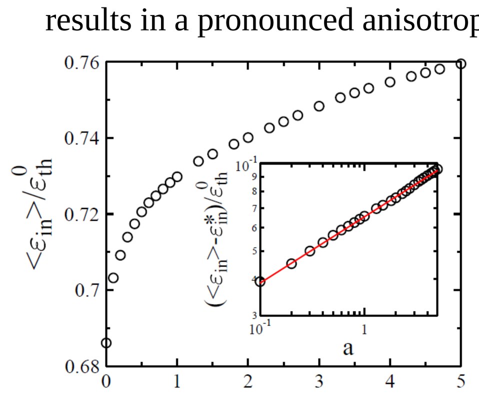

To charactize how crack initiation is affacted by the presence of anisotropy, we determined the average value $\langle\varepsilon_c\rangle$ of the shrinkage strain ε_{in} where the first microcrack nucleate in the system. The good quality straight line observed in the inset of Fig. 6 confirms that the crack initiation strain has a power law dependence on the degree of anisotropy $\langle\varepsilon_{in}\rangle = \varepsilon_{in}^* + Ba^{\beta}$.

Fig. 6. The average value of the shrinkage strain $\langle\varepsilon_c\rangle$ where the first crack nucleate in the layer scaled with the breaking parameter ε_{th}^0 as a function of the degree of anisotropy.

Three phases of cracking

When a beam breaks, a microcrack is formed along the common edge of the two polygons. As shrinking proceeds additional microcracks nucleate and gradually grow by the breaking of adjacent beams resulting in extended macrocracks. To obtain a clear view on the structure of the evolving crack pattern, we worked out an algorithm which constructs the macrocracks of the layer starting from individual microcracks. A macrocrack is identified as a continuous path of polygon edges with broken beams spanning between two junction points. A junction point of the crack network is a polygon corner from which either one, or three microcracks start. Polygon corners where two microcracks meet are considered to be internal points of macrocracks, while junctions of one and three microcracks are end points of arrested cracks, and the merging points of independent cracks, respectively (see Fig. 7).

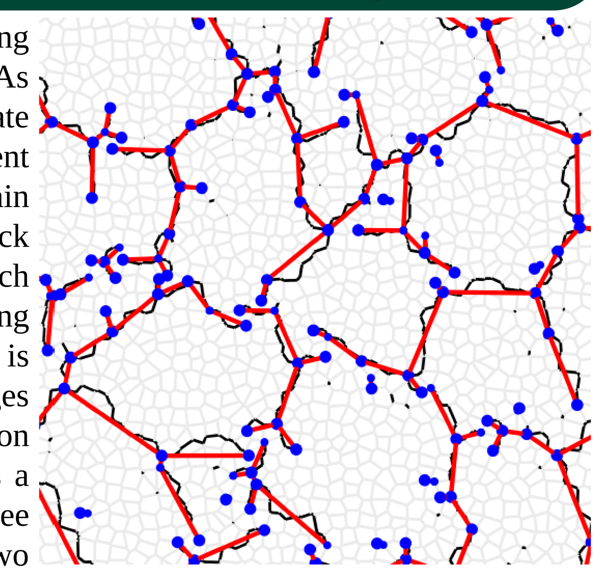

Fig. 7. Identification of junction points (blue dots) and macrocracks (straight red lines connecting junctions) in a snapshot of the damaged layer for the isotropic case $a = 0.0$.

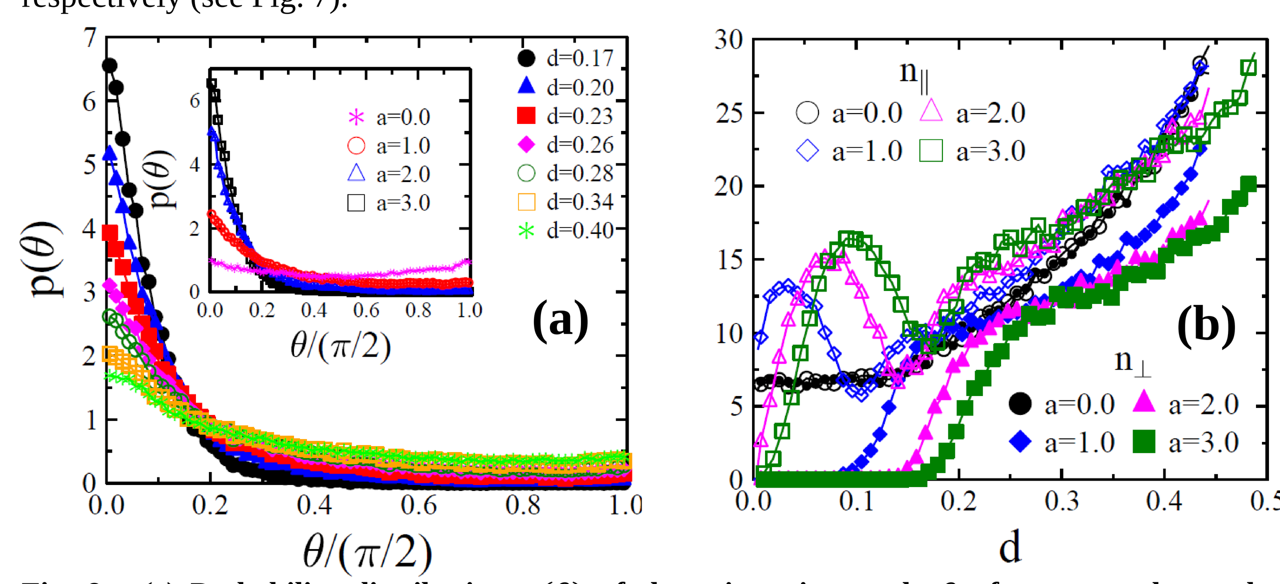

Fig. 8. *(a)* Probability distribution $p(\theta)$ of the orientation angle θ of macrocracks at the anisotropy $a = 3.0$ for several values of the damage fraction d. Inset: the distribution $p(\theta)$ for several degrees of anisotropy obtained at the same damage fraction $d = 0.17$. *(b)* Increments of the number of cracks of different directions as function of the damage fraction d at different anisotropies.

Macrocracks are characterized by their orientation, which is determined as the angle θ between the axis x and the straight line connecting the two end junctions of the crack. The probability distribution $p(\theta)$ of the orientation angle θ is presented in Fig. 8(a) for an anisotropic system $a = 3.0$ at several values of the damage fraction d. Angular distributions obtained at different degrees of anisotropy a are compared in the inset of Fig. 8(a) at the same value of the damage fraction $d = 0.17$ at an early stage of breakup. The strong effect of anisotropy on the crack orientation is evident, i.e. the distribution is nearly uniform for the case of isotropy $a = 0.0$, however, increasing a suppresses cracks at large angles, e.g. in case of $a = 3.0$ in the layer at this d value. We determined the increments of the number of cracks of different directions (Fig. 8(b)). We found that anisotropy $a > 0$ results in a clear separation of the increments for low d. To give a quantitative charazterization of the emergence of a connected crack network, we determined average mass of fragments (Fig. 9).

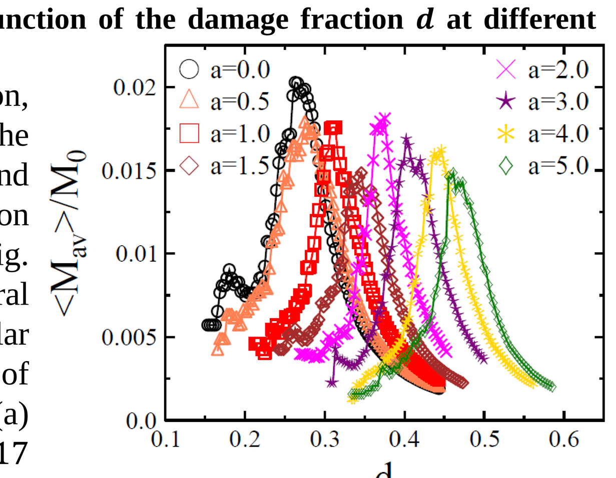

Fig. 9. Average mass of fragments as a function of the damage fraction for several values of the anisotropy parameter.

Based on the analysis of the crack orientation and of the overall structure of the emerging crack network we conclude that the evolution of the crack pattern has essentially three phases: *(I)* Primary cracking is dominated by the formation of long cracks aligned with a direction impronted by the initial mechanical excitation. *(II)* Secondary cracking sets on when cracks even perpendicular with the primary ones are generated. As desiccation proceeds, primary and secondary cracks merge which leads to *(III)* the emergence of connected network of cracks (see Fig. 10)

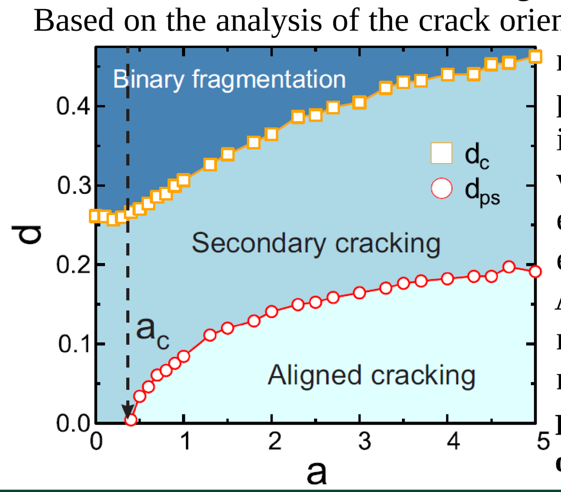

Fig. 10. The three phases of desiccation induced cracking on the damage-anisotropy parameter plane.

Binary fragmentation

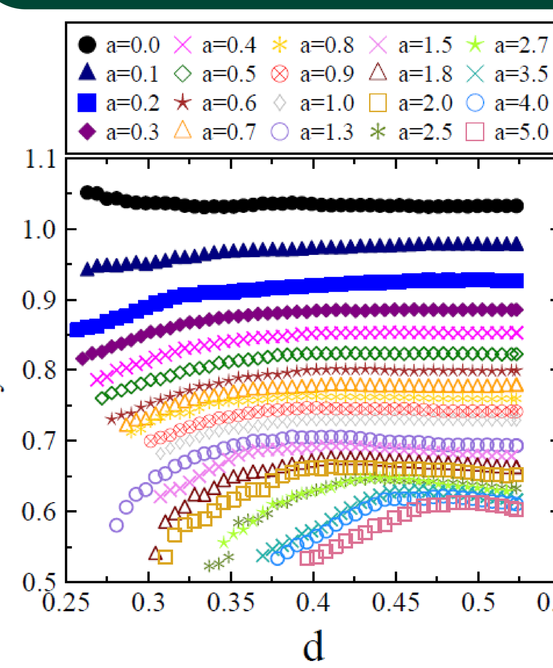

Fig. 11. The average aspect ratio $\langle L_y/L_x\rangle$ of fragments as a function of the damage fraction d for several anisotropies a. Note that the asymptotic value of the aspect ratio decreases with a.

The emergence of the connected crack network which spans the entire system has the consequence that layer breaks up into large number of fragments. We have seen that the structure of the crack network strongly depends on the degree of anisotropy, hence, it can be expected that anisotropy affects also the evolution of the fragmentation process. The long straight cracks of primary cracking create elongated slices in the layer, which are then segmented by the secondary cracks into smaller pieces. This mechanism results in fragments whose elongated shape originates from the structure of the connected crack network. To characterize the shape of fragments we determined the bounding box of individual pieces with side length L_x and L_y directed along the x and y axis of the initial coordinate system, respectively. It can be observed in Fig. 11 that in the absence of initial anisotropy $a = 0.0$, fragments have an isotropic shape $\langle L_y/L_x\rangle \approx 1$ at any damage state. However, anisotropy $a > 0$ of the local materials' strength gives rise to an elongated fragment shape.

The mass distributions $p(m,d)$ of fragments obtained at different damages d have a robust functional form (Fig. 12). Rescaling the mass distributions by the average fragment mass, the $p(m)$ curves of different d can be collapsed on a master curve. The data collapse implies the scaling structure of the distributions,

$$p(m,d) = \langle m\rangle^{-1}\psi(m/\langle m\rangle).$$

The scaling function $\psi(x)$ can be very well described by the log-normal distribution

$$\psi(x) = \frac{1}{x\sigma\sqrt{2\pi}} exp[-(\ln(x) - \mu)^2/2\sigma^2]$$

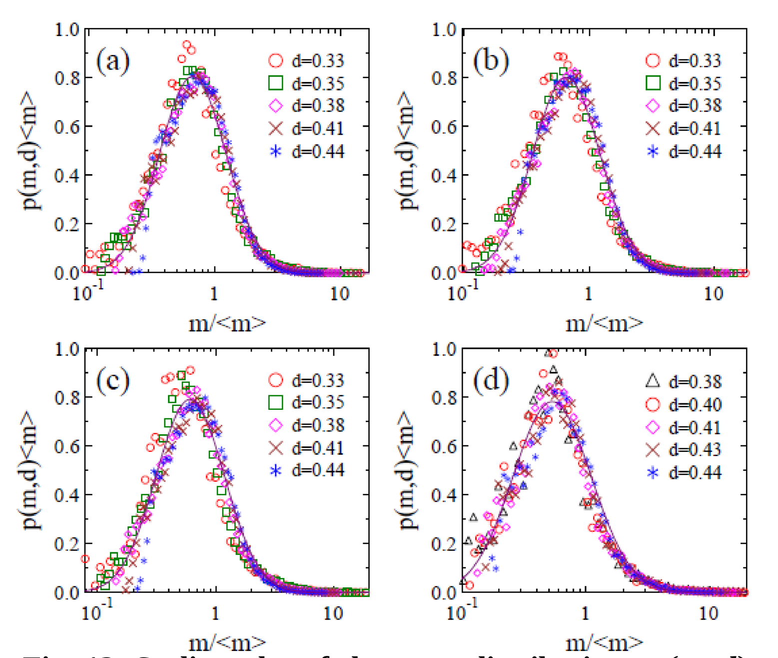

Fig. 12. Scaling plot of the mass distributions $p(m,d)$ of fragments at four different anisotropies: *(a)* $a = 0.0$, *(b)* $a = 0.5$, *(c)* $a = 1.0$ and (d) $a = 2.0$.

Conclusions

- In our study, cracking is found to evolve through three distinct phases of random nucleation and growth of cracks aligned with the strong direction, secondary cracking in the perpendicular direction, and finally binary fragmentation following the formation of a connected crack network.
- The anisotropic crack pattern gives rise to fragments with a shape anisotropy which gradually gets reduced as binary fragmentation proceeds.
- The statiscs of fragment masses exhibits a high degree of robustness which can be described by a log-normal functional form at all anisotropies.

Acknowledgement

The work is supported by the EFOP-3.6.1-16-2016-00022 project. The project is co-financed by the European Union and the European Social Fund.

References

- L. Goehring, A. Nakahara, T. Dutta, S. Kitsunezaki, and S. Tarafdar, *Desiccation Cracks and Their Patterns: Formation and Modelling in Science and Nature* (John Wiley & Sons, 2015).
- A. Nakahara, and Y. Matsuo, *Transition in the pattern of cracks resulting from memory effects in paste*, Phys. Rev. E 74, 045102 (2006).
- K. H. Nam, I. H. Park, and S. H. Ko, *Patterning by controlled cracking*, Nature 485 (2012).
- Z. Halász, A. Nakahara, S. Kitsunezaki, and F. Kun, *Effect of disorder on shrinkage-induced fragmentation of a thin brittle layer*, Phys. Rev. E 96, 033006 (2017).

Corresponding author: Ferenc Kun, email: ferenc.kun@science.unideb.hu